Journal of Advanced Sciences and Engineering Technologies (2025); 8(1):1-24

DOI: http://doi.org/10.32441/jaset.8.1.5

Journal of Advanced Sciences and Engineering Technologies

www.jasetj.com

Journal of Advanced Sciences and Eng. Technologies

JASET

The Effect of Varying Maximum Aggregate Size and Reinforcement Ratio on the Behavior of Reinforced Shear Key Specimens with Normal Steel Under Direct Shear

Raed Mokhalad Radeef*, Saad M. Raoof, Shagea Alqawzai[b]

[a] Civil Engineering Dept./ College of Engineering/Tikrit University /Tikrit, Iraq.

[b] Singapore Institute of Technology, One Punggol Coast Road, 828608, Singapore.

Keywords:

Dilation, direct Shear, Longitudinal Steel Reinforcement, Maximum Aggregate Size, Shear Capacity and Slip.

Highlights:

- Inverse Impact of Aggregate Size Based on Reinforcement Density: Increasing the maximum aggregate size positively influences shear capacity when the reinforcement ratio is at its minimum. However, conversely, when the reinforcement ratio is at its maximum, increasing the aggregate size leads to a decrease in shear capacity due to reduced spacing in the critical shear plane.
- Reinforcement Ratio Limitations: Increasing the longitudinal reinforcement ratio from minimum to maximum effectively increases shear capacity only when using small aggregates (2 mm). When using larger aggregates (9 mm), increasing the reinforcement ratio to the maximum actually results in a reduction of capacity.
- Ductility and Stiffness Consistency Regardless of the aggregate size or reinforcement ratio, all specimens demonstrated acceptable ductility, maintaining shear capacity even after 4 mm of slip. Additionally, all specimens maintained a similar stiffness slope up to peak capacity, attributed to the consistent modulus of elasticity of the reinforcement.

ARTICLE INFO

Article history:

Received	08 Aug	2024
Received in revised form	15 Dec	2024
Accepted	31 Dec	2024
Final Proofreading	10 Oct	2025
Available online	20 Oct	2025

*Corresponding author:

Raed Mokhalad Radeef

Civil Engineering Dept./ College of Engineering/Tikrit University /Tikrit, Iraq.

Abstract:

When designing concrete structural members subjected to different types of stresses, it is essential to optimize the contribution of all structural components. In the design of shear reinforcement for beams, the contribution of longitudinal bars to shear resistance is typically neglected, as they are mainly intended to resist bending stresses. This study investigates the influence of varying the longitudinal reinforcement ratio and maximum aggregate size on the behavior of shear key specimens. The experimental program includes nine specimens, incorporating three maximum aggregate sizes (2 mm, 4 mm, and 9 mm) and three reinforcement ratios (minimum, average, and maximum). After performing the required tests, the shear stress, slip, and dilation values were determined and compared among the specimens. The results demonstrated that increasing the maximum aggregate size enhanced the shear capacity when the reinforcement ratio was at its minimum. Conversely, when the reinforcement ratio was increased to its maximum level, the shear capacity decreased with increasing aggregate size.

INTRODUCTION

Concrete is generally reinforced to withstand tensile stresses due to its inherently low tensile strength. These tensile stresses can be categorized into those induced by bending and those induced by shear forces. Concerning the tensile stresses arising from shear forces, structural elements must possess the ability to endure these stresses to maintain their structural integrity. This capability is provided by their resistance to shear stress.

Generally, the shear resistance of a structural member consists of two important factors: the shear resistance of the steel, represented by the symbol Vs, and the shear resistance of the concrete, represented by the symbol Vc. According to (ACI code 318-14), determining the shear resistance of concrete is through a test called push-off specimens.

Various types of specimens are used for experimental investigations into the mechanisms of shear transfer; the push-off test specimen is the most employed for studying the influence of direct shear stresses.

The shear resistance of concrete is calculated based on three fundamental variables: the compressive strength of the concrete (Vcz), the aggregate size (Viy), and the reinforcement ratio used in the region subjected to direct shear in the push-off specimen's test. Therefore, the contribution of concrete to resisting shear forces is achieved through the combination of compressive strength, aggregate interlock, and the dowel action of the main reinforcing (Vd). (ACI Code 318-19). Figure 1 illustrates the shear forces acting on a reinforced beam to resist such forces, in addition to the contribution of the three influencing variables on the shear resistance of concrete.

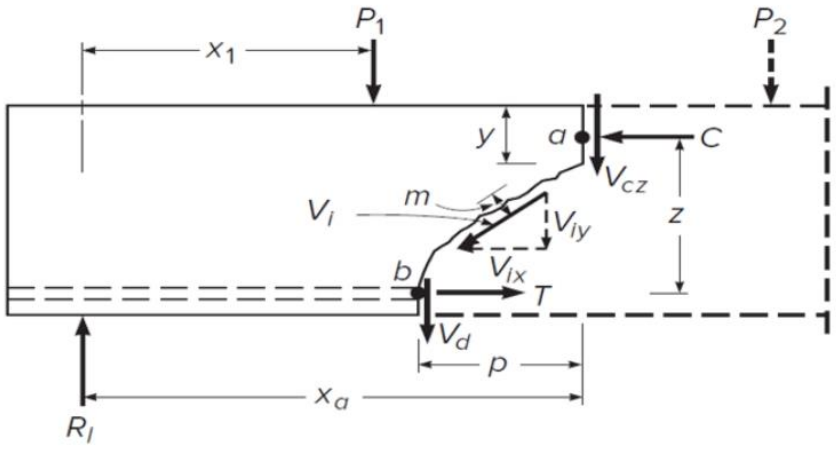

Figure 1 Forces at a diagonal crack in a beam without web reinforcement (Birkeland, 1966).

The shear resistance of concrete for any structural member can be calculated using the following equation:

$V_c = V_{cz} + V_{iy} + V_d$ (ACI 318-19, 22.5.1.1)

Where:

V_{cz} = Shear strength of concrete in the compression zone.

V_{iy} = Interface shear due to aggregate interlock along the cracks.

V_d = Dowel action force resistance of longitudinal reinforcement.

The primary factor influencing concrete shear resistance is the dowel action of steel reinforcement. Dowel action encompasses three distinct mechanisms: flexure, shear, and kinking of the steel bars, as illustrated in Figure 2. While significant levels of slip and concrete crushing are required to engage the reinforcement bars effectively, dowel action alone cannot be considered the primary mechanism for shear force resistance. Excessive slip can lead to deflection issues, and the development of prominent cracks in a reinforced concrete structure can be a significant concern for its occupants. Under typical load and slip conditions, it is estimated that only 15% of the shear-friction capacity is attributed to dowel action (Paulay et al., 1974).

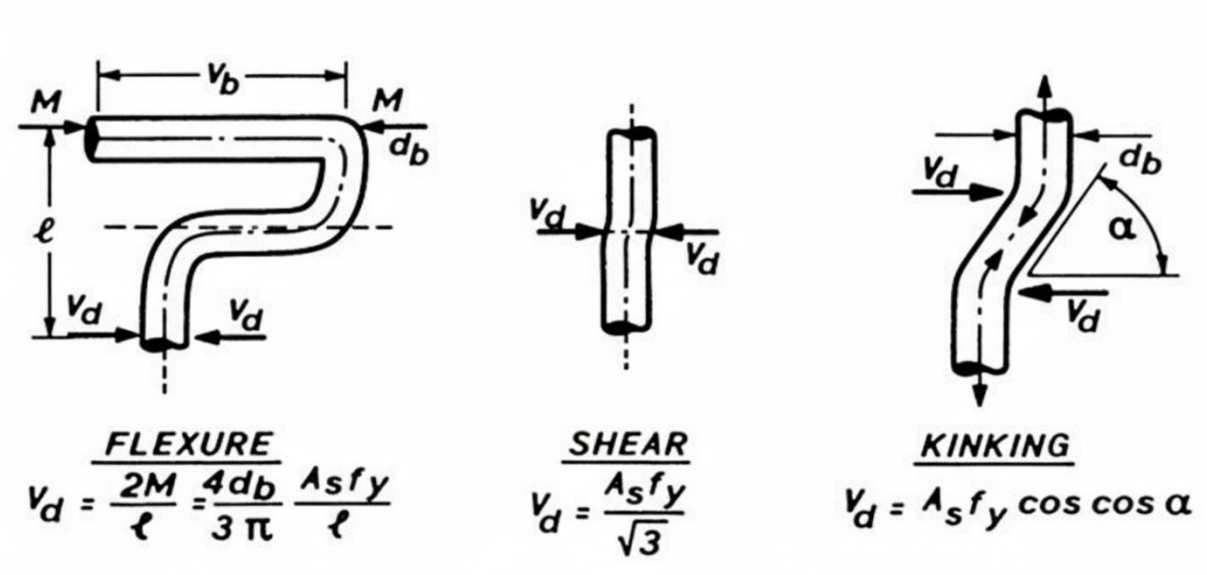

Figure 2 Mechanisms of dowel action (Paulay et al., 1974).

When utilizing standard steel reinforcement to reinforce concrete members exposed to relatively high shear forces, the contribution of the dowel force resistance of longitudinal reinforcement (V_d) is significant and effective due to the favorable properties of steel, such as ductility. This contrasts with the shear reinforcement resistance (V_{iy}), which is relatively lower due to the limited interaction between concrete and steel reinforcement caused by the relatively large spacing between the reinforcement bars, assuming the compressive strength of concrete remains constant.

(Khayat & Feys, 2010) examined the behavior of Steel Fiber-Reinforced Concrete (SFRC) through a series of experimental tests conducted. The study of shear behavior involved monitoring crack opening and shear displacement in relation to the shear load. The study variables included the type of concrete (either Self-Compacting Concrete (SCC) or SFRC with varying fiber contents: 40 kg/m3 or 60 kg/m3), transverse reinforcement (TR), and the width of the pre-crack. The analysis focused on aggregate interlocking, with the findings indicating that fiber inclusion improved failure control and enhanced ductility in shear response.

(Shariatmadar et al., 2013) Experimentally examines the shear transfer behavior in reinforced concrete through the testing of pre-cracked push-off specimens. The study concentrates on the quantity of reinforcement and the application of externally bonded fiber-reinforced polymer (FRP) fabrics along the shear plane. The findings of this study detail the shear transfer capacity and failure patterns of pre-cracked reinforced concrete push-off specimens that have been externally bonded with FRP.

(Al-attar, 2016) Examines the behavior of self-compacting concrete (SCC) at connection points under direct shear, with a focus on carbon fiber reinforcement effects externally. The findings indicate that carbon fiber addition enhances direct shear strength. However, exclusive use of carbon fiber resulted in brittle failure.

(Al-Quraishi et al., 2018) Investigate carried out both experimental and theoretical studies on the behavior of connections under direct shear, considering the influence of steel fiber reinforcement on the connections' strength and behavior. The study focused on the fiber content and the amount of shear reinforcement perpendicular to the shear plane. Data such as slip, lateral separation, and strains in the reinforcements and concrete were monitored.

In this study, normal steel reinforcement will be replaced with Carbon Fiber Grid (CFG) in the reinforcement of the region exposed to shear in push-off specimens. This is done to understand the effect of changing the type of reinforcement on the shear resistance of concrete. Since CFG consists of multiple openings with relatively uniform sizes, the interaction or bonding with concrete is expected to be very strong. Consequently, it is anticipated that the value of (Viy) will be greater than its counterpart when using normal steel reinforcement. On the other hand, it is also expected that the value of (Vd) will be very small due to the flexible nature of the CFG. Therefore, this study aims to determine which of the two different types of reinforcement has a greater effect on improving the shear resistance of concrete (Vc).

EXPERIMENTAL PROGRAM

The experimental program includes the following:

Material Properties Used in Experimental Program

Various materials, including Portland cement, fine aggregate, coarse aggregate, water, and steel bars, were utilized to create a mixture for shear key specimens in direct shear tests. Subsequent sections will detail the experimental tests performed on each material to verify its adherence to Iraqi standard specifications and ASTM standards.

Cement

Ordinary Portland Cement from the Tasloga factory, sourced from the local market, was used in this study. Physical and chemical tests were conducted in the laboratories of the College of Engineering at Tikrit University. The results of these tests demonstrate that the cement complies with the requirements of the Iraqi specifications (IQS NO. 5, 1984).

Fine Aggregate

The study utilized natural fine aggregate. The sieve analysis, sulfate content, and fine materials tests were conducted in the civil engineering laboratory at Tikrit University. A sieve size of 2.36 mm was used to obtain the fine aggregate passing for the second mortar mixture, with a Maximum Aggregate Size (M.A.S) of 2.36 mm. The test results met the requirements of the Iraqi standard specifications (I.Q.S. No. 45, 1984).

Coarse Aggregate

For the concrete mixture preparation, a coarse aggregate with a maximum size of 9.5 mm was utilized. The sieve analysis results, along with the coarse aggregate's sulfate content and fine materials, were performed at Tikrit University's civil engineering department. These test outcomes complied with the Iraqi Specification (I.Q.S. No. 45, 1984) requirements.

Water

Ordinary tap water was utilized for the mixing and curing processes.

Design of Concrete and Mortar Mixtures

The design includes the following:

Concrete Mixtures Design

Concrete mixes were designed to determine the appropriate proportions of the ingredients to achieve the required compressive strength of 40 MPa, in accordance with the ACI code (ACI PRC-211.1-91, 2009), using normal coarse aggregate of 9.5 mm. The proportions of this mix are detailed in Table 1.

Table 1: Proportions of mixture design.

Mix NO.	Proportions	Cement (kg/m^3)	Sand (kg/m^3)	Gravel (kg/m^3)	W/C (kg/m^3)	W/C %
1	1: 1.63: 2.10	445	725	935	205	46%

Mortar Mixtures Design

Thirteen mortar mixtures were suggested to select suitable proportions of the mix ingredients that satisfy the required compressive strength of 40 MPa in the present study. The mortar mixture has 2 variables: W/C and three cements and sand content variables in 2 different M.A.S of sand, namely, 4.75mm and 2.36 mm. The proportions of this mix are shown in Table 2.

Table **2** : Trail Mix for Mortar.

Mix NO.	Proportions	Cement (kg/m^3)	Sand 4.75 mm(kg/m^3)	Sand 2.36 mm(kg/m^3)	W/C (kg/m^3)	W/C %
1	1: 1	400	400	0	160	0.42
2	1:1.5	400	600	0	160	0.42
3	1: 2	400	800	0	160	0.42
5	1: 1	400	400	0	180	0.45
6	1: 1.5	400	600	0	180	0.45
7	1: 2	400	800	0	180	0.45
8	1: 1	400	0	400	160	0.42
9	1: 1.5	400	0	600	160	0.42
10	1: 2	400	0	800	160	0.42
11	1 :1	400	0	400	180	0.45
12	1:1.5	400	0	600	180	0.45
13	1: 2	400	0	800	180	0.45

Reinforcements

Base Reinforcement and Ties for Shear Key Specimens (steel bars)

This study employed two types of deformed reinforcing steel bars: Ø12 mm diameter bars for base reinforcement and Ø10 mm diameter bars for reference specimens in direct shear tests. The tensile test results for these reinforcement bars are provided in Table 3.

Table 3 The tensile test results of the reinforcement steel bars.

Diameter (mm)	Yield stress (Fy) (MPa)	Ultimate strength (Fu) (MPa)
10	416	633.52
12	427	657.38

Strain Gauge

A strain gauge is a device used to measure the strain or deformation of an object. The sensor converts mechanical displacement or strain into an electrical signal. Strain gauges are commonly used in various applications such as stress analysis, load measurement, and force sensing.

Oasis Technology, Inc., manufactured the strain gauge, and Tokyo Measuring Instruments Lab manufactured the epoxy adhesive and SB tape for protection and coating materials, as shown in Figure 3.

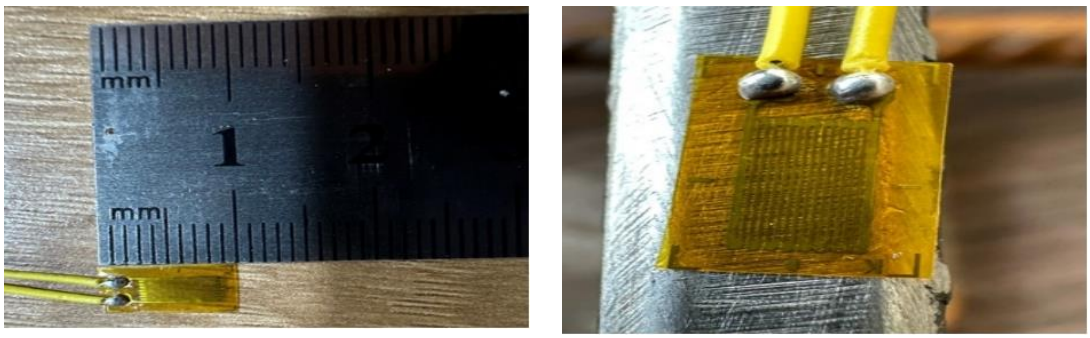

(a) (b)

Figure 3 Steel Strain gauge used in the current study.

The properties of the strain gauge, adhesive materials, SB tape, and coating material (W-1) are shown according to the manufacturer's datasheet Table 4**.**

Table 4 Properties of the steel strain gauge used in the current study according to the manufacturer's data.

SG	*No.*	*1*	*2*	*3*	*4*	*5*	*6*
BF120-5AA	Details	hxw	bxh	Gauge resistance	Sensitivity coefficient	Wire length	Transverse sensitivity
Steel – one direction	Description	5x2	9.6 x 4	120/350 ± 0.1Ω	2.08 ± 1% (A level)	2.5 m	-0.6%

Molds preparations

The 9-shear key specimens were cast using wooden molds. 3 molds were prepared, with 3 specimens cast for each of the three mixtures. The dimensions of the molds were 600 mm in height, 300 mm in width, and 150 mm in depth (Samantha Lynn Wermager, 2015), as illustrated in Figure 4

Figure 4: The wooden molds used in the current study.

Details of Specimens

This study used 9 shear key Specimens with dimensions of 600 × 300 × 150 mm (height, width, and depth, respectively). Table 5 shows the specimen matrix. These samples were divided into three groups, each containing 3 samples, according to the type of mixtures used. The first mixture was a cement mortar with a maximum size of 2.36 mm. The second mixture was a cement mortar with a maximum aggregate size of 4.75 mm. The third mixture was normal concrete with a maximum aggregate size of 9.5 mm. Each group included one reinforced model with normal steel rebars, serving as reference models with three reinforcement ratios: ρ_{min}, $\rho_{av.}$, and $\rho_{max.}$ These specimens were tested in a direct shear test (Push-off Test).

The shear plane area for the shear key models was 32,400 mm², with the reinforcement ratios chosen as 0.009, 0.016, and 0.022. All details are shown in Table 6 and Figure 5.

Table 5: Specimens Matrix details

Mix Type	Mortar 2.36 mm			Mortar 4.75 mm			Normal Concrete 9.5 mm		
Reinforcement ratio(ρ)	0.009	0.016	0.22	0.009	0.016	0.22	0.009	0.016	0.22
Specimen ID	M2-1	M2-2	M2-3	M4-1	M4-2	M4-3	NC-1	NC-2	NC-3

Note on names for specimens: - Xn-Y

X-type of concrete mix

N- M.A.S, 2 for 2.36 and 4 for 4.75 mm (mortar mixture)

C: M.A.S. 9.5 mm (normal concrete)

Y-type of reinforcement:

1, 2, and 3 for (Steel rebars)

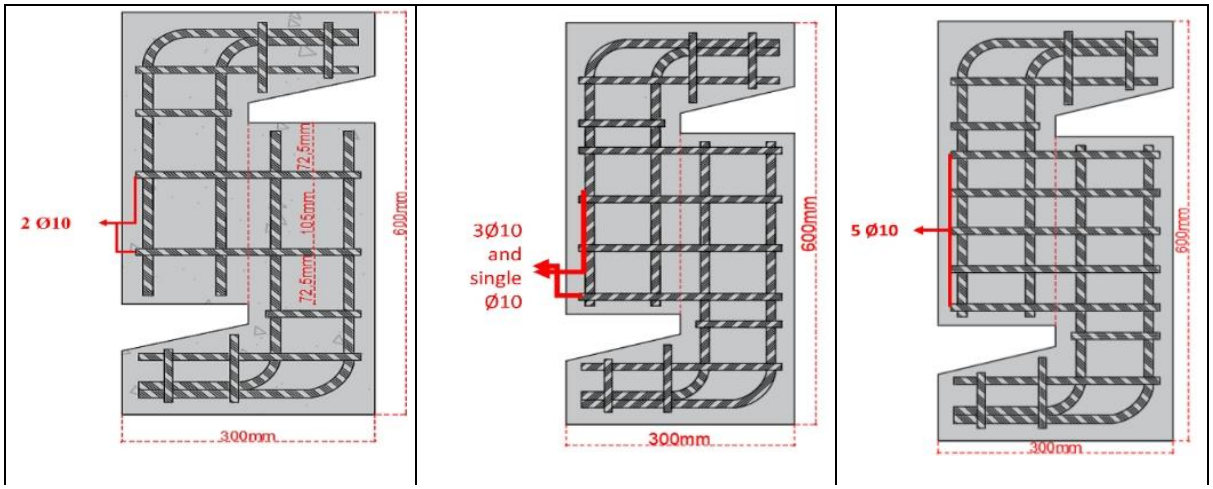

(a)ρ_{min} (M2-1, M4-1, NC-1) ρ_{ava}, (M2-2, M4-2, NC-2) ρ_{max}(M2-3, M4-3,NC-3)

Figure 5 Details of all specimens' reinforcement (a) steel- specimens

Preparing, casting, and curing of shear key specimens

All mixture components were prepared using an electronic balance in the graduate laboratory at Tikrit University's College of Engineering. Two types of laboratory mixers were used to mix the components for two varieties of cement mortar and one type of normal concrete. All wooden molds were primed and oiled, and the reinforcement of shear key specimens was arranged within them, as illustrated in Figures 6 and 7. The casting process involved filling the molds with the mixture and compacting the samples using a mechanical vibrator. After pouring, the concrete and the top surfaces of all main shear key specimens were smoothed with a hand steel trowel, as shown in Figure 8. A groove was then made on the upper surface of the direct shear zone, corresponding to the incision on the lower surface initially installed in the model, as shown in Figure 9. These grooves are useful for forcing cracks to form at the designated location of the specimens. Samples were de-molded 24 hours post-casting and subsequently cured in water. Finally, all specimens were painted white to enhance the visibility of crack formation and growth during tests, as shown in Figure 10.

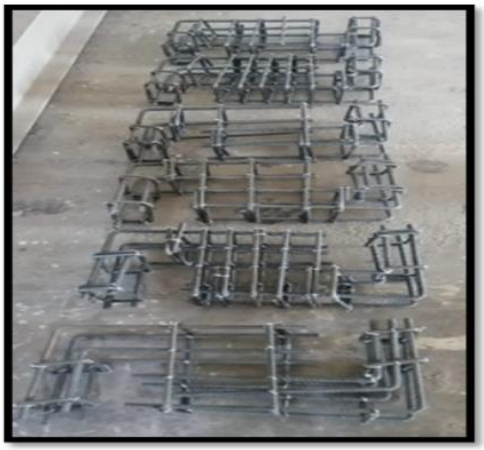

Figure 6 Reinforcement of the shear key specimens.

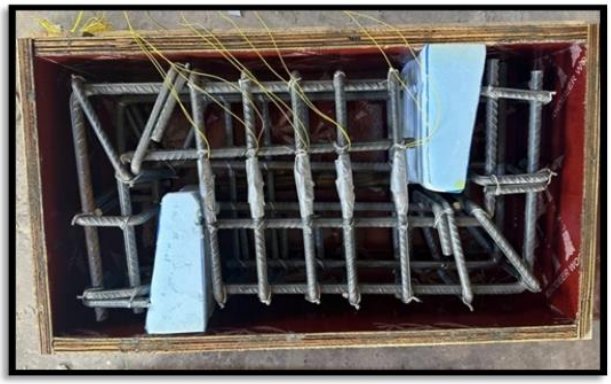

Figure 7: Preparation of molds and reinforcement placed in molds of the shear key specimens.

Figure 8 Casting, vibrator for compact, finished the surface by hand steel trowel of the shear key specimens.

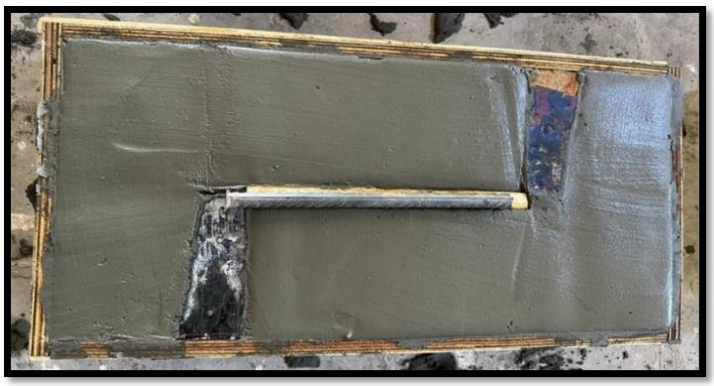

Figure 9 (a) making a groove in specimens after refining the top face.

Figure 10 Painted shear key specimens.

Test setup

A universal testing machine (UTM), specifically a SANS model with a capacity of 2000 kN, was employed for the test. The load was applied at a rate of 1.5 kN/sec. The specimens were subjected to two-point loading. The force exerted was measured using a load cell, along with six Linear Variable Differential Transformers (LVDTs).

Two LVDTs were placed on the right and left sides, touching the top and bottom adjustments to measure the vertical displacement (slip) of the specimens. Additionally, four LVDTs were installed, with two on each face of the specimen, to measure the crack width (dilation). A data logger with 16 channels was used to collect data from the test, as illustrated in Figures 11 and 12.

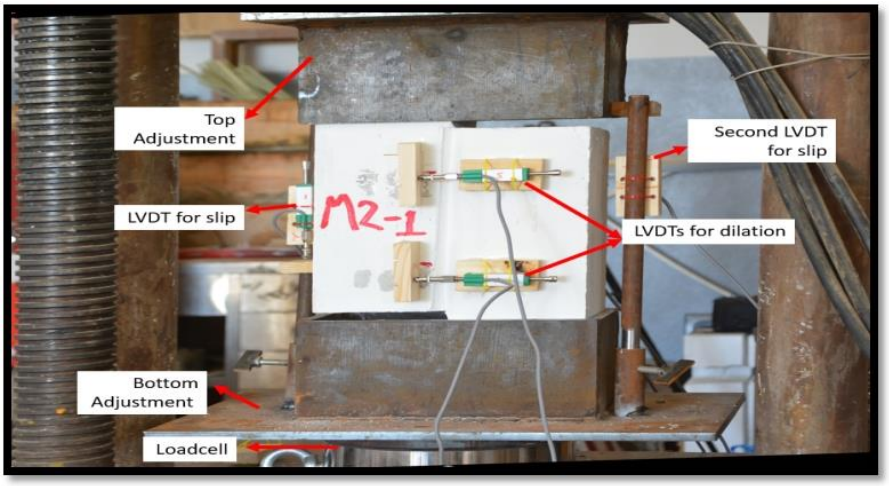

Figure 11 Load and deflection monitoring by the data logger.

Figure 12 Load and deflection monitoring by the data logger.

Experimental Results

Specimens with Longitudinal Steel Reinforcement

The recorded data regarding the shear key specimens with longitudinal steel reinforcement tested in this study includes nine specimens, with three maximum aggregate sizes with three longitudinal reinforcement ratios.

Specimens with min reinforcement ratio (ρ = ρmin)

The results of testing the shear key specimens with longitudinal steel reinforcement with a reinforcement ratio of 0.009 are presented in Figure 13. All specimens showed failure along the critical shear plane as was planned.

(a) (b) (c)

Figure 13 Shear plane crack of specimens with minimum steel reinforcements, a) maximum aggregate size of 2.36 mm, b) maximum aggregate size of 4.75 mm, and c) maximum aggregate size of 9.5 mm.

As shown in Figure 14, the shear resistance of the examined specimens clearly increased with the increase of maximum aggregate size in the used concrete. Shear key

with maximum aggregate size of 9 mm resisted shear force equal to 461 kN compared to 416 and 376 kN for specimens with maximum aggregate size of 4 and 2 mm, respectively, which represent an increase of 11% and 23% respectively. This behavior was expected and attributed to the larger contribution of the aggregate interlock factor (V_{iy}) in the total concrete shear capacity (V_c).

In terms of the slip at the ultimate shear, it was almost similar for all examined specimens with different maximum aggregate sizes. This behavior was attributed to the similarity in the amount of steel reinforcement that contributed the same amount of resistance due to the dowel action in the longitudinal bars (V_d), as well as the similar kinking deformations due to the similarity in the stiffness of the deformed longitudinal bars .

As for the ductility of the examined specimen with minimum longitudinal steel reinforcement, the result showed a decent ductility, where the specimen with maximum aggregate size of 9 mm maintained a shear capacity of 201 kN at slip of 4 mm, which represents 44% of the ultimate shear capacity. This clear ductility is fully attributed to the ductile nature of the main steel reinforcement that can endure noticeable deformations after the yielding point, unlike other brittle materials.

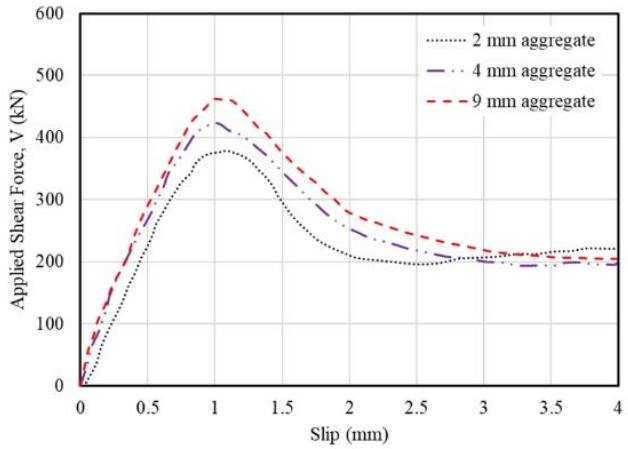

Figure 14 Recorded shear force vs. vertical slip for specimens with longitudinal steel reinforcement; with $\rho = \rho_{min}$.

A similar trend was noticed with the crack width versus the applied shear force, as shown in Figure 15, which represents the horizontal crack width (Dilation) versus the applied shear force. The relation was almost linear up to the peak shear capacity, then moved to nonlinear behavior due to the yielding in the steel reinforcement. Since all of the examined specimens in this group have the same amount of longitudinal steel reinforcement with the same stiffness, both the dealation at the ultimate shear force

and the slope of the curve were almost identical. In addition, the ductility was very clear as well.

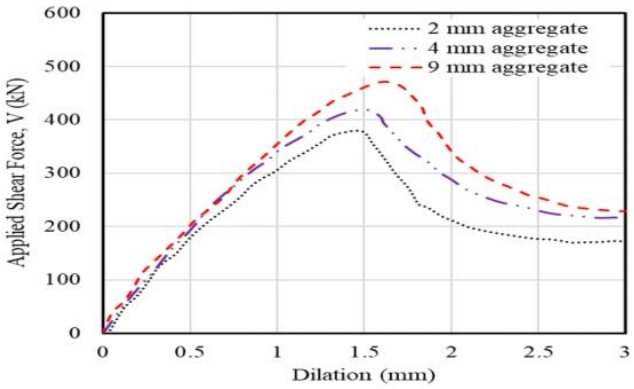

Figure15 Recorded shear force vs. horizontal dilation for specimens with longitudinal steel reinforcement; with $\rho = \rho_{min}$.

Figure 16 represents the relation between the slip and dilation. Due to the High ductility nature of the rest Theory reinforcement, this figure shows that as much as you increase the slip, the dilation, which represents the crack, the horizontal crack width increases until a crack width of 3 mm is recorded. At this level of dilation, all of the specimens showed a slip range from 4 mm in a specimen with a 9 mm maximum aggregate size to 3 mm in a specimen with a 2 mm maximum aggregate size.

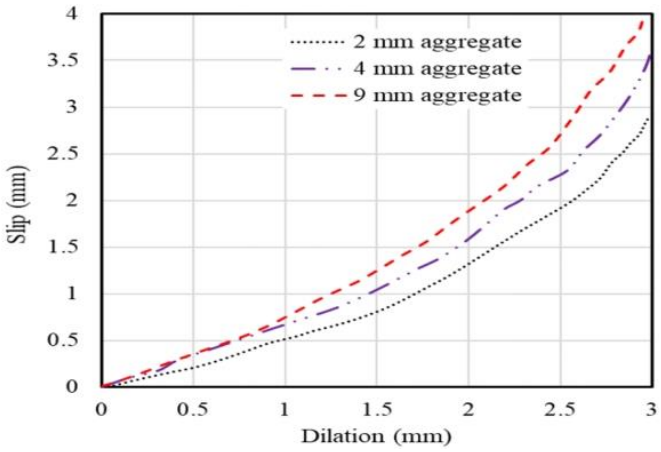

Figure 16 Slip vs. dilation for specimens with longitudinal steel reinforcement; with ρ = ρmin.

Specimens with average reinforcement ratio ($\rho = \rho_{average}$)

The results of testing of the shear key specimens with longitudinal steel reinforcement with a reinforcement ratio of 0.016 are summarized in Figure 17.

(a) **(b)** **(c)**

Figure 17 Shear plane crack of specimens with average steel reinforcements: a) maximum aggregate size of 2 mm, b) maximum aggregate size of 4 mm, and c) maximum aggregate size of 9 mm.

As shown in Figure 18, the shear receptance of the test specimens was almost similar with the increase of maximum aggregate size in the used concrete. Shear keys with maximum aggregate size of 2-, 4-, and 9-mm resisted shear force ranged between 490 and 510 kN. This vanishing of the contribution of the aggregate interlock factor (V_{iy}) in the total concrete shear capacity (V_c) was due to the relatively reinforcement-crowded zone of the critical shear section, which obstructed the equal arrangement and flow of the aggregate, especially the one with a maximum size of 9 mm. This led to reducing the shear capacity to a one similar to that in small aggregate size, which can flow and arrange in a better way due to the smaller size of aggregate.

In terms of the slip at the ultimate shear, it was almost similar for all examined specimens with different maximum aggregate sizes. This behavior was attributed to the similarity in the amount of steel reinforcement that contributed the same amount of resistance due to the dowel action in the longitudinal bars (V_d), as well as the similar kinking deformations due to the similarity in the stiffness of the deformed longitudinal bars. However, the slip of specimens with an average reinforcement ratio was smaller than that with the minimum reinforcement ratio due to the increased resistance that came from increased contribution of the dowel action of longitudinal bars.

As for the ductility of the examined specimen with average longitudinal steel reinforcement, the result showed a notable ductility where the specimen with a maximum aggregate size of 9 mm maintained a shear capacity of 150 kN at slip of 4 mm, which represents 30% of the ultimate shear capacity. This ductility is attributed

to the ductile nature of the main steel reinforcement that can endure noticeable deformations after the yielding point, unlike other brittle materials.

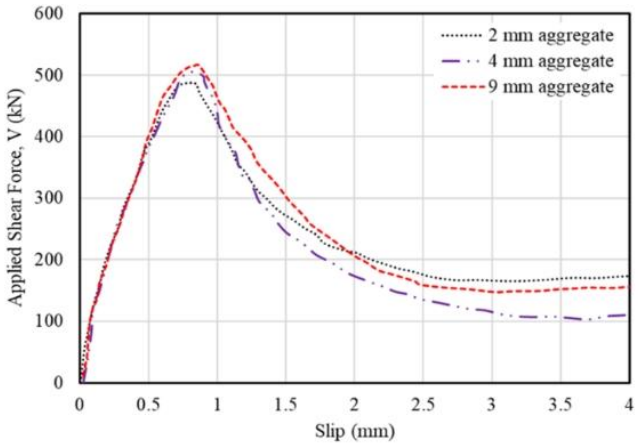

Figure18 Recorded shear force vs. vertical slip for specimens with longitudinal steel reinforcement; with $\rho = \rho_{average}$.

A similar trend was noticed with the crack width versus the applied shear force, as shown in Figure 19, which represents the horizontal crack width (Dilation) versus the applied shear force. The relation was almost linear up to the peak shear capacity, then moved to nonlinear behavior due to the yielding in the steel reinforcement. Since all of the examined specimens in this group have the same amount of longitudinal steel reinforcement with the same stiffness, both the dealation at the ultimate shear force and the slope of the curve were almost identical. In addition, the ductility was very clear as well.

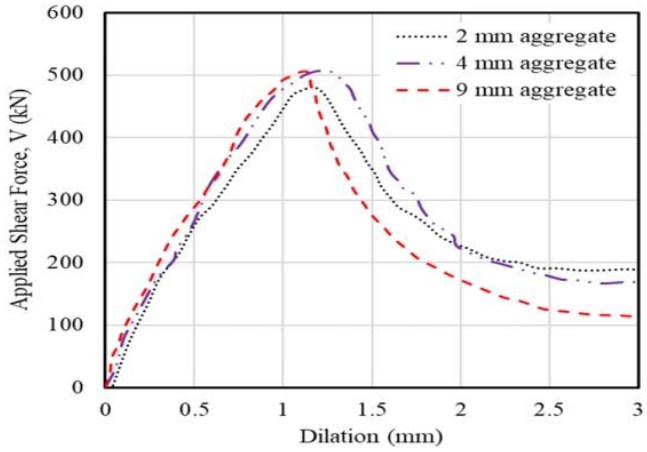

Figure19 Recorded shear force vs. horizontal dilation for specimens with longitudinal steel reinforcement; with $\rho = \rho_{average}$.

Figure 20 represents the relation between the slip and dilation. Due to the High ductility nature of the rest Theory reinforcement, this figure shows that as much as

you increase the slip, the dilation, which represents the crack, the horizontal crack width increases until a crack width of 3 mm is recorded. At this level of dilation, all of the specimens showed a slip range from 4 mm in a specimen with a 9 mm maximum aggregate size to 2.5 mm in a specimen with a 2 mm maximum aggregate size.

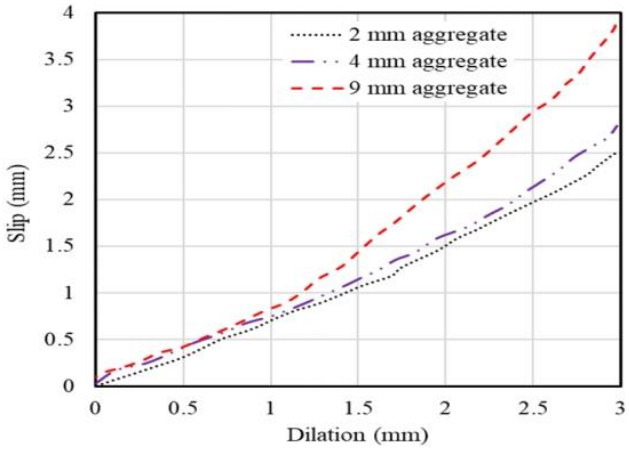

Figure 20 Slip vs. dilation for specimens with longitudinal steel reinforcement; with $\rho = \rho_{average}$.

Specimens with max. reinforcement ratio ($\rho = \rho_{max}$)

The results of testing of the shear key specimens with longitudinal steel reinforcement with a reinforcement ratio of 0.022 are summarized in Figure through Figures. All specimens showed failure along the critical shear plane as was planned (Figure 21).

(a) (b) (c)

Figure 21. Shear plane crack of specimens with max. Steel reinforcements: a) maximum aggregate size of 2 mm, b) maximum aggregate size of 4 mm, and c) maximum aggregate size of 9 mm. Unlike the previous two cases, in this case with the maximum reinforcement ratio, specimens with a maximum aggregate size of 2 mm

showed the highest shear resistance capacity, which contradicts the assumption or the hypothesis that a higher or larger maximum aggregate size results in higher shear capacity. This phenomenon can be attributed to the heavily reinforced crowded zone at the critical shear section, which totally prevented the aggregate from interfering in the critical zone and worked almost as a sieve to prevent large particles from going inside. In addition, the encapsulation around the steel bars, which has a direct connection to the bond, where affected as well. As a result, this produced less capacity for a specimen with concrete that has a relatively larger aggregate size. As shown in Figure 22, the shear resistance of the test specimens was increased with the decrease of maximum aggregate size in the used concrete. Shear key with maximum aggregate size of 2 mm resisted shear force equal to 570 kN compared to 500 and 420 kN for specimens with maximum aggregate size of 4 and 9 mm, respectively, which represent a decrease of 14% and 26% respectively. This behavior was attributed to the prevention of the aggregate from entering the critical zone due to the high reinforcement, which reduced the contribution of the interlock factor (V_{iy}) in the total concrete shear capacity (V_c). In terms of the slip at the ultimate shear, it was almost similar for all examined specimens with different maximum aggregate sizes. This behavior was attributed to the similarity in the amount of steel reinforcement that contributed the same amount of resistance due to the dowel action in the longitudinal bars (V_d), as well as the similar kinking deformations due to the similarity in the stiffness of the deformed longitudinal bars.As for the ductility of the examined specimen with maximum longitudinal steel reinforcement, the result showed a noticeable ductility where the specimen with maximum aggregate size of 2 mm maintained a shear capacity of 260 kN at slip of 4 mm, which represents 46% of the ultimate shear capacity. This clear ductility is fully attributed to the ductile nature of the main steel reinforcement that can endure noticeable deformations after the yielding point, unlike other brittle materials.

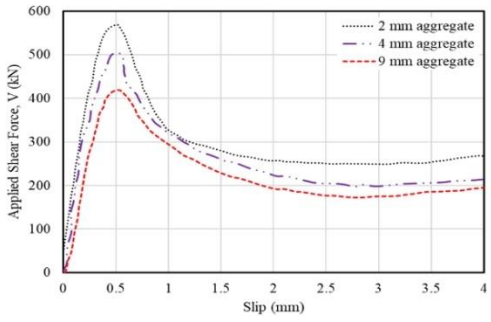

Figure 22 Recorded shear force vs. vertical slip for specimens with longitudinal steel reinforcement; with $\rho = \rho_{max}$.

A similar trend was noticed with the crack width versus the applied shear force, as shown in the Figure, which represents the horizontal crack width (Dilation) versus the applied shear force. The relation was almost linear up to the peak shear capacity, then moved to nonlinear behavior due to the yielding in the steel reinforcement. Since all of the examined specimens in this group have the same amount of longitudinal steel reinforcement with the same stiffness, both the dealation at the ultimate shear force and the slope of the curve were almost identical. In addition, the ductility was very clear as well.

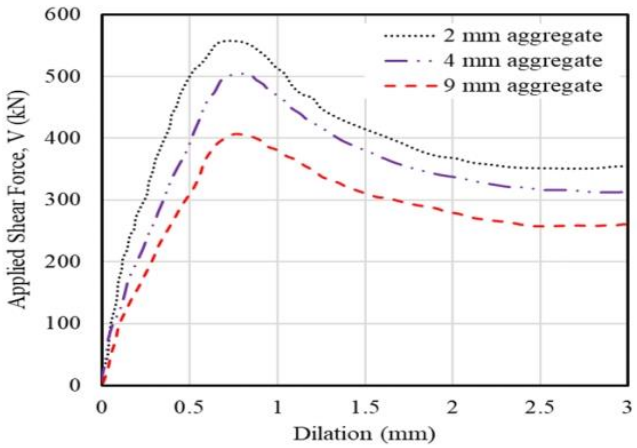

Figure 23 Recorded shear force vs. horizontal dilation for specimens with longitudinal steel reinforcement; with $\rho = \rho_{max}$.

Figure **24** represents the relation between the slip and dilation. Due to the high ductility nature of the steel reinforcement, this figure shows that as much as you increase the slip, the dilation, which represents the horizontal crack width, increases until a crack width of 1.7 to 2.5 mm is recorded. At this level of dilation, all of the specimens showed a slip of around 1.5 mm followed by full collapse due to concrete crushing as a result of the high reinforcement ratio.

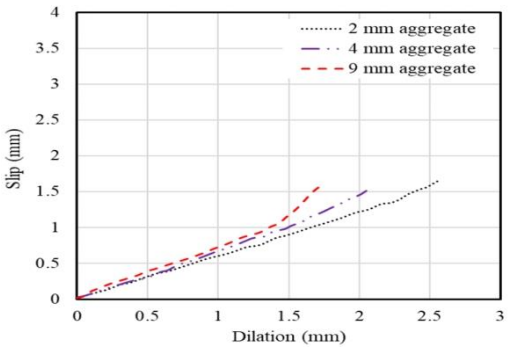

Figure 24 Slip vs. dilation for specimens with longitudinal steel reinforcement; with $\rho = \rho_{max}$.

Effect of Reinforcement Ratio

Figure 25 showed a comparison between the different reinforcement ratios that were examined in this study for steel reinforcement by presenting the shear capacity of all examined specimens reinforced with different maximum aggregate sizes and reinforcement ratios. As shown in all figures, increasing the reinforcement ratios increases the shear capacity of the tested specimens only the relatively small aggregate size of 2 mm, while decreasing the shear capacity in the case of specimens with 4 and 9 mm maximum aggregate sizes. The small aggregate size of 2 mm helped to highlight the impact of increasing the reinforcement ratio for steel. However, with a relatively large aggregate size of 9 mm, increasing the reinforcement ratio decreased the shear capacity due to the prevention of the large aggregate particles from reaching the critical shear plane due to the small spacing between the steel bars. For example, shear keys reinforced with steel bars showed an improvement in the shear capacity of 50% when the reinforcement ratio was increased from minimum to maximum with a maximum aggregate size of 2 mm. However, with max. Aggregate size of 9 mm, the shear capacity decreased by 10% when the reinforcement ratio was increased from min to max due to the reason that was explained before.

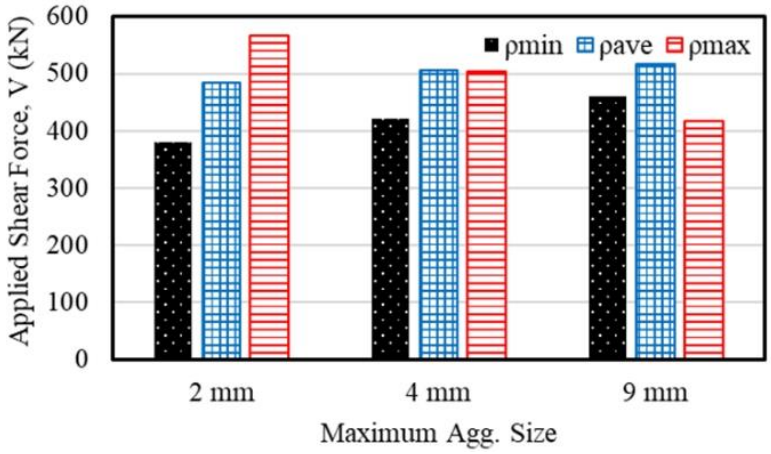

Figure 25 Shear capacity of all examined specimens with different maximum aggregate sizes and reinforcement ratios.

Effect of Aggregate Size

Figure 26 showed a comparison between all of the examined shear keys with different maximum aggregate sizes of 2-, 4-, and 9-mm with different reinforcement ratios that were used in this study by presenting the shear capacity of all examined specimens .

As shown in the figure, increasing the maximum aggregate size helped in increasing the shear capacity when the reinforcement ratio was the minimum. For example, shear

keys with steel reinforcement and a minimum reinforcement ratio showed an increase in the shear capacity of 22% when the maximum aggregate size increased from 2 to 9 mm. While at the maximum reinforcement ratio, increasing the maximum aggregate size to 9 mm caused a decrease in the shear capacity. For example, shear keys with maximum reinforcement ratio decrease in the shear capacity by 27% when the maximum aggregate size increases from 2 to 9 mm. The reason behind this significant difference in the shear capacity was attributed to the heavily reinforced crowded zone at the critical shear section, which totally prevented the aggregate from interfering in the critical zone and worked almost as a sieve to prevent large particles from going inside. In addition, the encapsulation around the steel bars, which has a direct connection to the bond, where affected as well. As a result, this produced less capacity for a specimen with concrete that has a relatively larger aggregate size. This behavior eliminated the aggregate interlocking factor (V_{iy}) for the shear capacity equation and resulted smaller shear capacity value (V_c).

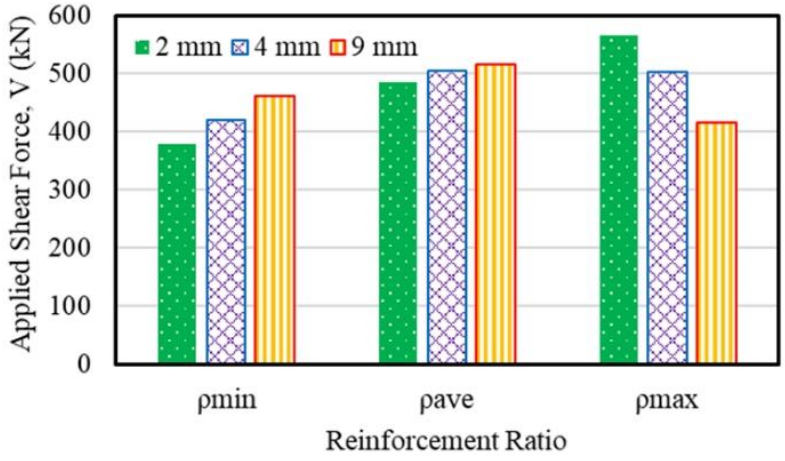

Figure 26 Shear capacity of all examined specimens with different maximum aggregate sizes and reinforcement ratios.

CONCLUSION

1- Specimens showed higher shear capacity ranging between 65 and 84% with a minimum reinforcement ratio and a maximum aggregate size of 2 mm. This impact was more pronounced with a higher maximum aggregate size. This behavior was attributed to the significant contribution of the steel bars, which can resist kinking as well as direct shear.

2- All specimens showed acceptable ductility by maintaining noticeable shear capacity after 4 mm of slip. This can be attributed to the ductile nature of steel reinforcement.

3- Regarding the stiffness and the crack opening of all of the specimens, all of them always maintained the same slope until the peak shear capacity. This can be attributed to the similarity in the modulus of elasticity of reinforcement.
4- Increasing the maximum aggregate size contributed positively to increasing the shear capacity when their reinforcement ratio was at the minimum. However, by increasing the reinforcement ratio to the maximum, the sheer capacity decreased with increasing the maximum aggregate size. This can be attributed to the small spacing that was available in the critical shear plane.
5- Increasing the reinforcement ratio from the minimum to the maximum helped in increasing the shear capacity when the maximum aggregate size was 2 mm. However, by using a maximum aggregate size of 9 mm, the capacity decreased with the increase in the maximum reinforcement ratio.

References

[1]American Concrete Institute (ACI. (2014). In Design and Construction Guide of Externally Bonded FRCM System for Concrete and Masonry Repair and Strengthening (ACI 549. American Concrete Institute.

[2]Al-Shathr, B. S., Al-Attar, T. S., & Hasan, Z. A. (2016). Effect of curing system on metakaolin based geopolymer concrete. Journal of Babylon University, 24(3), 569-576.

[3]Al-Quraishi, H., Lafta, M. J., & Abdulridha, A. A. (2018). Direct Shear Behavior of Fiber Reinforced Concrete Elements. Journal of Engineering, 24(1), 231–248. https://doi.org/10.31026/j.eng.2018.01.16

[4]Birkeland, P. W. B. and H. W. (1966). Connections in Precast Concrete Construction. ACI Journal Proceedings, 63(3). https://doi.org/10.14359/7627

[5]Iraqi Specification, No. 5/1984. Portland Cement. Central Agency for Standardization and Quality Control, Planning Council, Baghdad, Iraq.

[6]Iraqi Specification, No. 45/1984. Aggregate from Natural Sources for Concrete and Construction. Central Agency for Standardization and Quality Control, Planning Council, Baghdad, Iraq.

[7]Khayat, K. H., & Feys, D. (2010). Design, Production and Placement of Self-Consolidating Concrete. RILEM Bookseries, 1, 429–438. https://doi.org/10.1007/978-90-481-9664-7

[8]Paulay, T., Park, R., & Phillips, M. H. (1974). Horizontal construction joints in cast-in-place reinforced concrete. American Concrete Institute, ACI Special Publication, SP-042, 599–616. https://doi.org/10.14359/17303

[9]Samantha Lynn Wermager. (2015). Shear-friction of sand-lightweight clay and slate aggregate concretes with varied reinforcement ratios.

[10]Shariatmadar, H., Khatamirad, M., & Zamani, E. (2013). Pre-Cracked Concrete Shear Strengthened with External CFRP Strips. Journal of Rehabilitation in Civil Engineering, 1(1), 29–38.